



Research paper

Molecular dynamics simulation of the crystal structure evolution of titanium under different Tdamp values and heating/cooling rates

Juze Jiang^a, Xiaoxun Zhang^{a,*}, Fang Ma^b, Sensen Dong^a, Wei Yang^a, Minghui Wu^a^a School of Materials Engineering, Shanghai University of Engineering Science, Shanghai 201620, China^b School of Mechanical and Automotive Engineering, Shanghai University of Engineering Science, Shanghai 201620, China

ARTICLE INFO

Keywords:

Molecular dynamics

Ti

Temperature damping parameter

Heating/cooling rate

Crystal structure

ABSTRACT

Molecular dynamics (MD) was used to study the evolution of crystal structure of titanium (Ti) under different temperature damping parameter (Tdamp) values and heating/cooling rates. In the heating process, when the temperature reaches the melting point, the temperature of the system with larger Tdamp value decreases with the increase of average atomic potential energy. However, an increase in heating rate will cause the melting point to rise slightly. In the cooling process, a larger Tdamp value or a lower cooling rate is more conducive to the crystallization of Ti, which corresponds to the higher crystallization temperature.

1. Introduction

Titanium and its alloy have been widely used in aerospace, marine and medical fields due to their high strength ratio mechanical properties, excellent corrosion resistance and chemical compatibility [1–4]. However, it's poor materials-processing and components-manufacturing abilities for traditional manufacturing processing as known to all [5,6]. Fortunately, the emergence of new technologies, such as metal additive manufacturing (AM) technology, will overcome the problems caused by the difficulty of material processing. AM relies on its unique processing characteristics controlling laser/electron beam to melt metal powder fast then solidify quickly, which can greatly improve mechanical properties of materials [6–8]. Hence, great attention has been drawn for AM in industries in recent years. Nevertheless, the challenge of directly observing metal rapidly melting and solidification process remains, let alone characterize the evolution of crystal structure. Thereby, a workable way is required to research the evolution of crystal structure of metals during the rapidly heating/cooling process.

Molecular dynamics (MD) provides us an effective way to study the evolution of metal crystal structure from atom scale, which has been widely used to research crystallization of materials during solidification [9–12]. M. Azadeh et al. [13] utilized MD to study the distribution of surface energy and potential energy when the crystal structure of Pd nanoparticles transformation. S. Serzat et al. [14] researched the evolution of the crystal structure of Ag-Cu-Ni ternary nanoparticles during heating/cooling process by MD method. Furthermore, S. Kurian et al.

[15] studied the nucleation and growth of nano-Al particles in the molten pool during selective laser melting via MD simulation.

Based on the research ideas of predecessors, we utilized MD to research the evolution of the crystal structure of Ti under different Tdamp values and heating/cooling rates. The results show that the crystal structures have no obvious changes in the heating process, except for the sudden rise of disordered atoms ratio at the melting point. We believe that it will be another feasible way to judge melting point, where the ratio of disordered atoms rises suddenly. However, in the cooling process, the crystal structures show the great changes under different Tdamp values, which also appears in different cooling rates.

For the real situation of MD simulation, only one Tdamp value is suitable. Other values are not appropriate. In our work, four groups of Tdamp values were used to research the relationships between average atomic potential energy vs temperature and crystal structure ratio vs temperature. It is interpreted that the phenomenon of S-shaped change at average atomic potential energy vs temperature diagram during the heating process, which provides a reference to optimize Tdamp values to suit current simulation. Then, the optimized Tdamp value was utilized to research the evolution of crystal structure under different heating/cooling rates. The results show that a higher heating rate slightly rises the melting point of Ti. However, it's more conducive to the crystallization of disordered atoms (type of Other) at a lower cooling rate. Besides, there are some FCC (face-centered cubic) crystal structures transforming to HCP (close-packed hexagonal) structures during the solidification process.

* Corresponding author.

E-mail address: xxzhangsh@163.com (X. Zhang).

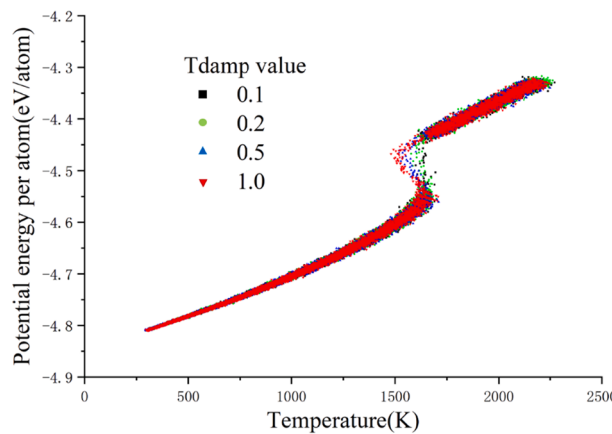


Fig. 1. Average atomic potential energy vs temperature diagram under different Tdamp values.

2. Computational methodology

2.1. Interatomic interactions

We utilized the embedded atom model (EAM) provided by G.J. Ackland [16] to simulate. This EAM describes the anisotropy of the shear constant and the deviation of the c/a lattice parameter ratio from the ideal value, while maintaining a smooth monotonic function. Moreover, G.J. Ackland (1987) and Finnis (1988) insisted that the potential energy function could be used for molecular dynamics simulation at finite temperature [16]. Compared with other EAM provided by M.I. Mendelev [17] and R.G. Hennig [18]. The EAM provided by G.J. Ackland deviates from reference value 1941 K in melting point [19], which is underestimated the stacking energy of I_2 dislocation in HCP. However,

the transition of crystal structure is continuous in the whole simulation process, and there is no instability of crystal structure in some specific temperature range [16]. After deliberate consideration, the EAM provided by G.J. Ackland was used to research the evolution of crystal structure of Ti in our work.

2.2. Simulation details

We used LAMMPS (large-scale atomistic/molecular massively parallel simulator) code for molecular dynamics simulation. Firstly, a square box of $10 \times 10 \times 10$ (unit of lattice constant) was established with periodic boundary conditions. The original structure of Ti is HCP at room temperature and zero pressure [20]. When the temperature reaches the 1941 K [19], Ti will completely melt. To ensure complete melting of titanium, the upper limit of heating temperature was set at 2200 K. Therefore, we studied the crystal structure changes from the stable state to disordered state in the temperature range of 300 K to 2200 K. First, the system was relaxed at 300 K for 20 ps in canonical (NVT) ensemble. Then, isothermal isobaric (NPT) ensemble was used to heat the system from 300 K to 2200 K. In the cooling process, the system was relaxed at 2200 K for 20 ps, then cooled down from 2200 K to 300 K. Finally, relaxing the system at 300 K for 20 ps and ending the simulation process. The energy minimization was utilized, and the time step was set as 1 fs. The whole simulation was carried out in a Nosé-Hoover thermostat environment. Within OVITO (the Open Visualization Tool), common neighbor analysis (CNA) was used to identify the local crystalline structure of atoms.

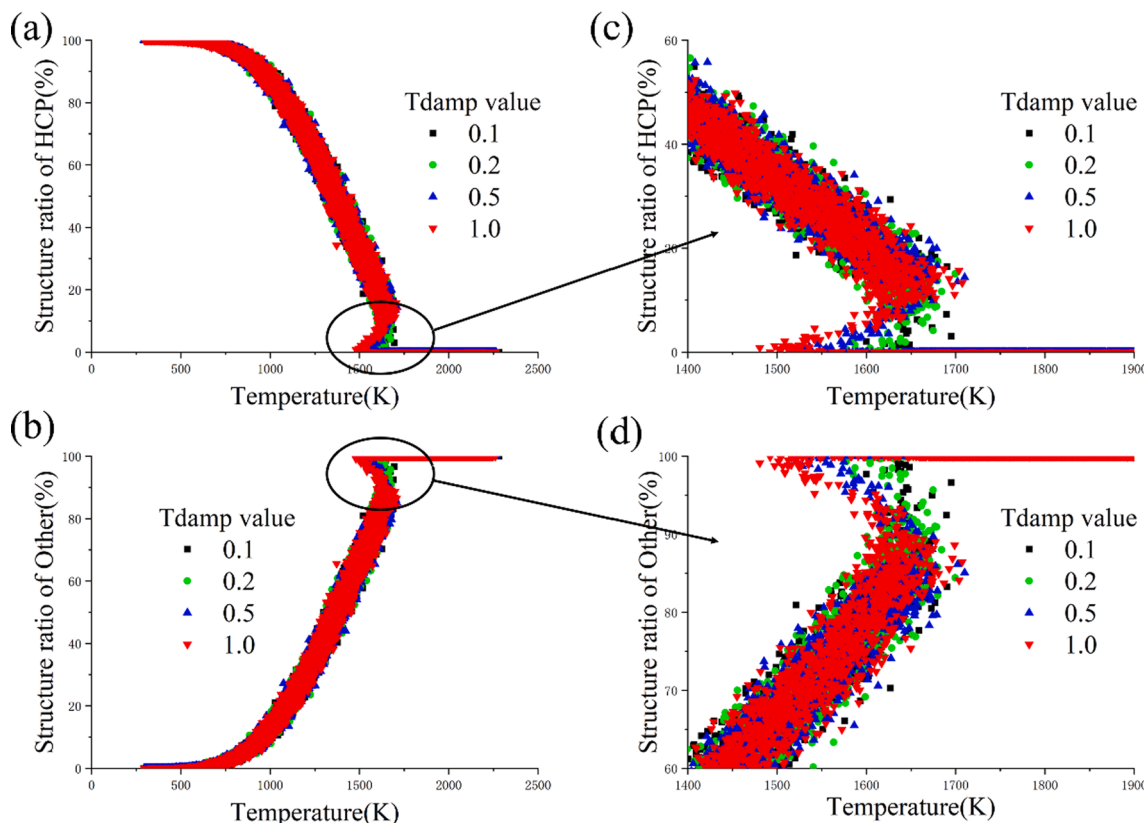


Fig. 2. (a, b) The crystal structure ratio vs temperature under different Tdamp values. (c, d) are an enlarged view of (a, b) at 1400–1900 K, respectively.

3. Results and analysis

3.1. Tdamp values

3.1.1. Influence of Tdamp values on crystal structure evolution and the melting point

The melting point is one of the important properties of metal materials, and is related to the first-order phase transition [20–22]. Crystalline materials undergo phase transitions to disordered state at the melting point when being heated [22]. Thereby, the structure evolution of the crystal can be used to research its melting behavior in the heating process. An increase of potential energy will happen between atoms during the heating process when the crystal structures transform to disordered state. Meanwhile, the issue of equilibrium of temperature in the system ought to be considered. Tdamp is specified in time units and determines how rapidly the temperature is relaxed. A Nosé-Hoover thermostat will not work well for arbitrary values of Tdamp. If Tdamp is too small, the temperature can fluctuate wildly; if it is too large, the temperature will take a very long time to equilibrate. Therefore, four groups of Tdamp values (0.1, 0.2, 0.5, 1.0) were set to research the evolution of crystal structure during the heating process, at which the heating rate kept consistent. The relationship between average atomic potential energy and temperature in each group of Tdamp value, as shown in Fig. 1.

From Fig. 1, it is found that in a larger Tdamp value's system, when the temperature reaches the melting point, the average atomic potential energy increases with the decrease of temperature. Moreover, The larger the Tdamp value, the more pronounced the temperature drop. Finally, the S-shaped phenomenon appears between potential energy and temperature at the melting point. Associating the change of crystal structure of the crystal endothermic transition to disordered atoms in the melting process, the crystal structure ratio vs temperature diagram is plotted, as shown in Fig. 2.

Fig. 2 (a, b) show that almost the same changing tendency for ratio of crystal structures under different Tdamp values. The main transformation of crystal structure is from HCP to Other in whole heating process, but near the melting point have slight difference. For careful observation, the enlarged picture of Fig. 2 (a, b) in the temperature range of 1400–1900 K is shown in Fig. 2 (c, d). From Fig. 2 (d), it is found that the temperature drops with the increase of the ratio of disordered atoms when the temperature reaches the melting point. What's more, the larger the Tdamp value is, the further offset value is away from the melting point, which is similar to Fig. 1. Next, the leftmost data points in Fig. 1 and Fig. 2 (d) were measured. Their corresponding temperatures are very close. In Fig. 1, the temperature from left to right is 1482.0 K, 1559.6 K, 1577.0 K and 1599.9 K, respectively. In Fig. 2, the temperature from left to right is 1480.3 K, 1559.4 K, 1578.7 K and 1599.5 K, respectively. Meanwhile, the temperature corresponding to the sudden change of crystal structure was measured, which average value is 1657.8 K. Compared with Fig. 1, it is close to the average temperature of 1658.7 K, which corresponds to the start jump point of average atomic potential energy.

As is known to all: the total energy in the system is composed of the total potential energy and total kinetic energy [23], the formula shows as following:

$$E_T = E_{(kinetic)} + E_{(potential)} \quad (1)$$

$$E_{(kinetic)} = \frac{3}{2} N \cdot k \cdot T \quad (2)$$

Where, in formula (1), E_T represents the total energy of the atom group, $E_{(kinetic)}$ is the total kinetic energy of the atom group, and $E_{(potential)}$ represents the total potential energy of the system. In formula (2), $E_{(kinetic)}$ represents the total kinetic energy of the atom group, N is the number of atoms in the group, k is Boltzmann's constant, and T

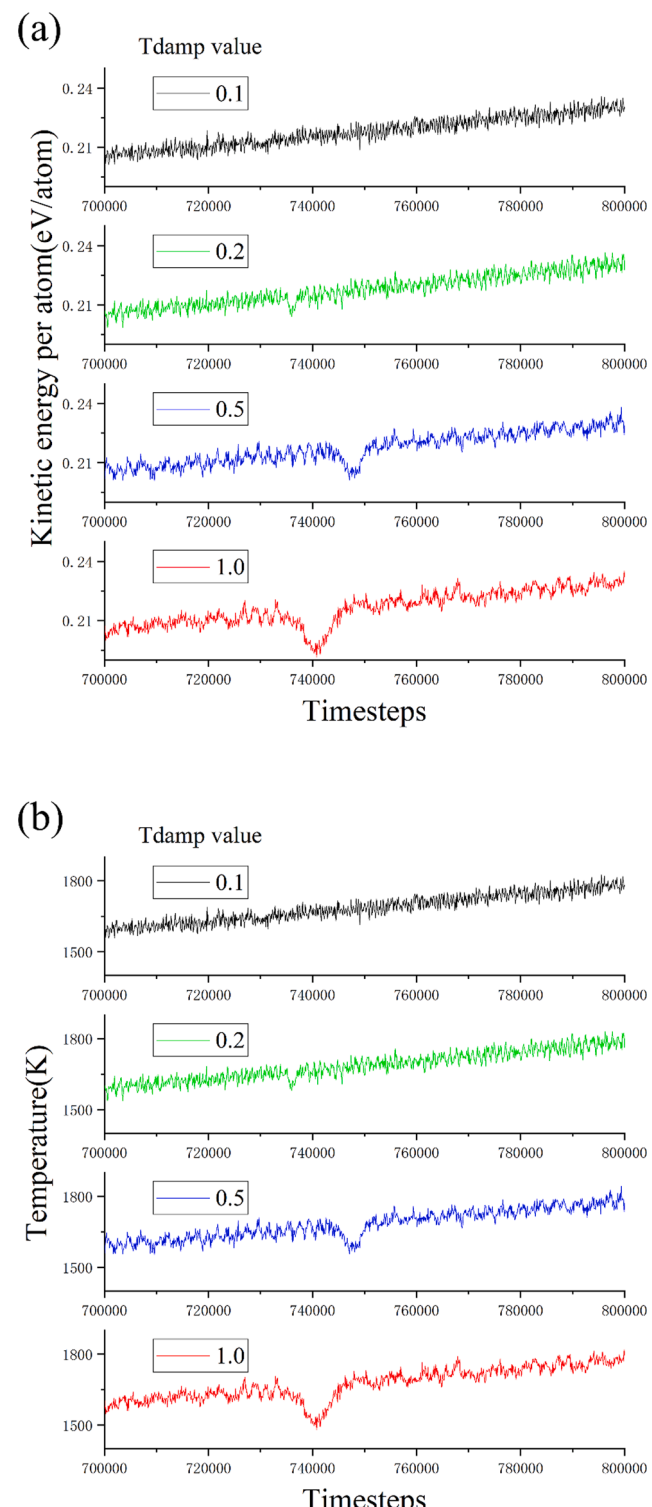


Fig. 3. (a) Atomic average kinetic energy vs timesteps diagram. (b) Temperature vs timesteps diagram.

represents the current temperature of the system. There is a linear relationship between system temperature and kinetic energy from formula (2). The average atomic kinetic energy and temperature vs their timesteps curves are shown in Fig. 3.

From Fig. 3, the results show that average atomic kinetic energy and temperature have the same trend over time, indicating that there is a linear relationship between temperature and kinetic energy. Fig. 3 (a) shows that in a larger Tdamp value system, the average atomic kinetic

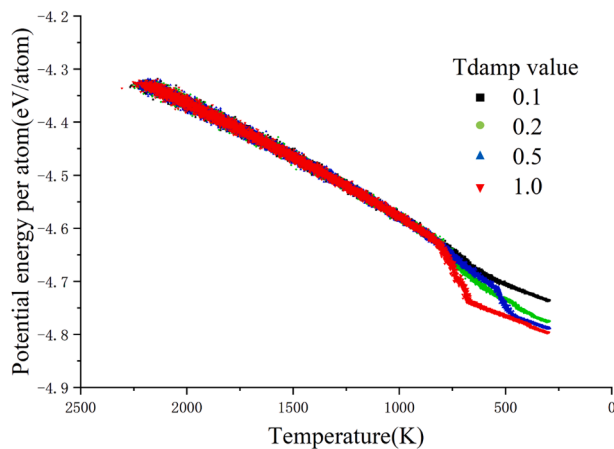


Fig. 4. Average atomic potential energy vs temperature diagram under different Tdamp values.

energy decreases significantly when the temperature reaches the melting point, corresponding to the time for temperature to reach equilibrium is prolonged in Fig. 3 (b). The explanation for this phenomenon is as follows: When the temperature reaches the melting point,

atoms with crystal structure need huge energy to break metal bonds to transform disordered states. In the system of 1.0 Tdamp value, it will take a longer time to equilibrate the temperature due to the heater can't supply enough energy to the atoms during the melting period. In this condition, the atoms will sacrifice their kinetic energy to give priority to satisfying their potential energy which results in the decrease of kinetic energy, corresponding to the temperature down. Only when the total energy provided by the heater is sufficient to meet the atomic demand during the melting process, will the kinetic energy recover, and maintains linearly with temperature.

No matter how the Tdamp value changes during the heating process, atoms at the melting point will absorb a lot of energy to satisfy its potential energy jump, causing the ratio of disordered atoms increases sharply. Consequently, the temperature of 1657.8 K can be judged as the melting point of Ti, at which the crystal structures change abruptly from HCP structure to Other structure. The results of simulation are various on melting point by different EAM. The melting points obtained by our simulation is close to the results obtained by W.S. Ko et al. [24] and Y.M. Kim et al. [25], which illustrates the feasibility and reliability of the simulation results. In most cases, the radial distribution function (RDF) is used to characterize the arrangement of atoms in many literatures [9,24–26], and to assist in judging the melting point of metals. However, it is worth mentioning that another feasible method is found to judge the melting point of metals from the evolution of crystal structure, where

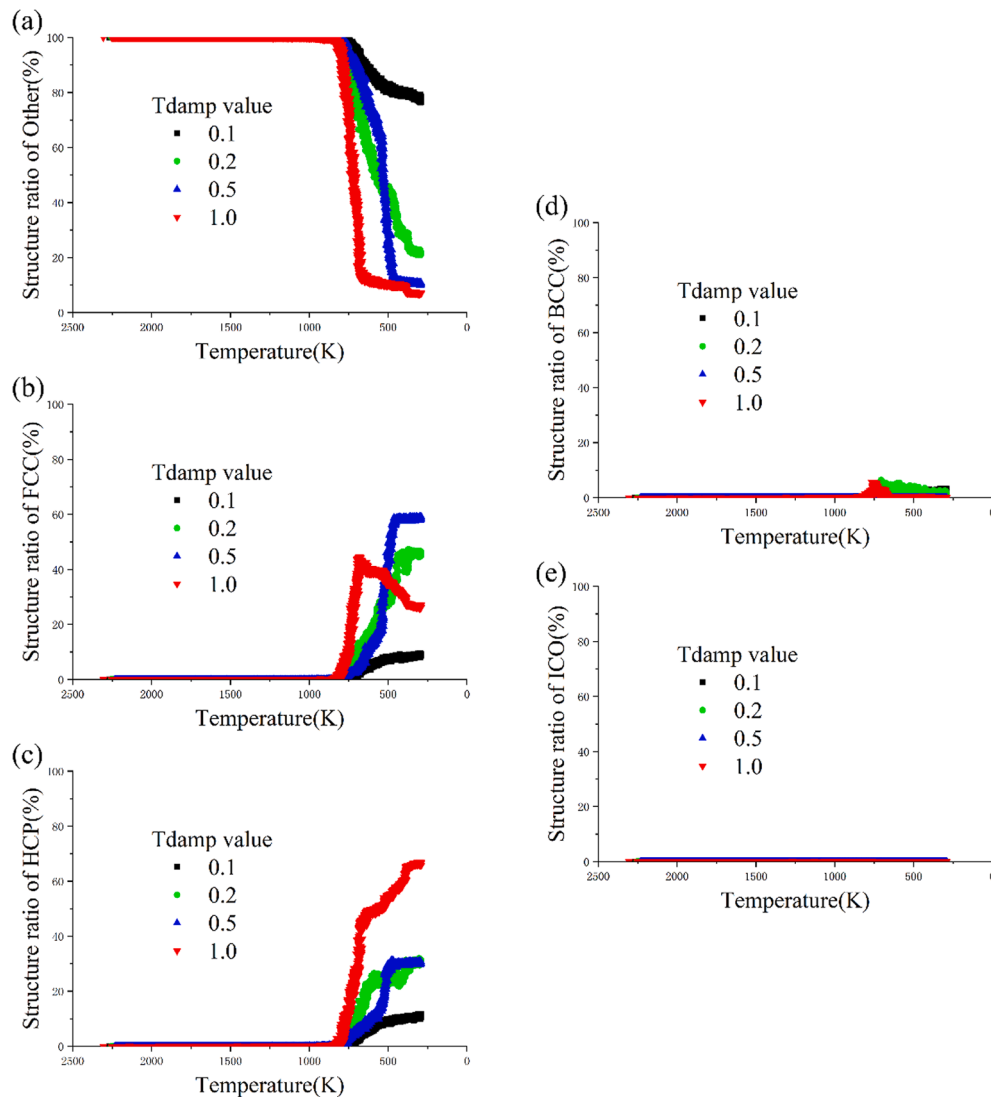


Fig. 5. The ratio of crystal structures ratio vs temperature diagram under different Tdamp values.

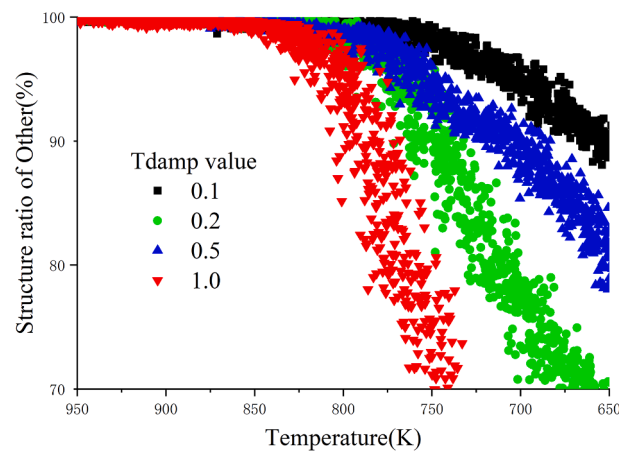


Fig. 6. Structure ratio vs temperature magnification diagram of the disordered atoms beginning to transform into crystal structure under different Tdamp values.

the ratio of crystal structure rises sharply from crystallization to disordered state.

3.1.2. Influence of Tdamp values on crystal structure evolution and the crystallization temperature

Crystallization is the approach of phase transition from liquid or gas to the solid, which consist of an arrangement of atoms [25]. It is great significance to predict the crystallization temperature of metals through phase transitions. In order to research the effect of different Tdamp values on evolution of crystal structures during the cooling process. First of all, it should be considered that the change of average atomic potential energy with temperature during the solidification process.

Fig. 4 shows that the larger the Tdamp value, the more obvious the decrease of average atomic potential energy during the solidification process, resulting in a lower average atomic potential energy of the system at 300 K. The change of average atomic potential energy means that different types crystal structures formed. Therefore, a deeply study is demanded on transformation of crystal structures from disordered atoms. The relationship between crystal structures ratio and temperature is shown in Fig. 5.

Fig. 5 shows that in a larger Tdamp values system, the disordered atoms are more likely to form crystal structures, and present a faster transformation speed during the solidification process. In the Tdamp value of 0.1 system, the crystal structures mainly transform from Other to FCC, HCP and BCC (body-centered cubic). After relaxation, the crystal structures and its ratio are FCC (8.8%), HCP (11.6%), BCC (2.2%), respectively. A lower transformation ratio is showed from disordered atoms to crystal structures in this condition. While increase the Tdamp value to 0.2, the transformation ratio greatly increases. Similarly, the mainly type of transformation is from Other to FCC and HCP. The ratio of BCC structures shows a trend of first increase and then decrease during the solidification process. After relaxation, the crystal structures and its ratio are FCC (45.9%), HCP (30.6%), BCC (1.6%), respectively. In the system of Tdamp value of 0.5, the transformation of crystal structures can be divided into two stages: slow first and then fast, and a large number of FCC (58.7%) and HCP (30.4%) structures are formed in the final system. Finally, while the Tdamp value up to 1.0, the ratio of BCC structures increases rapidly in a short temperature range and then decrease sharply. We infer that some BCC structures transformed to FCC and HCP structures during the solidification process, a similar phenomenon also appears in the paper of T. Abe et al [27]. In addition, FCC structures and HCP structures formed rapidly during the solidification process. When the ratio of FCC structure reaches the maximum value of 41.6% at 673.3 K, and then slowly decreases to 26.6%, but the structure ratio of HCP shows an upward trend in all solidification process. The

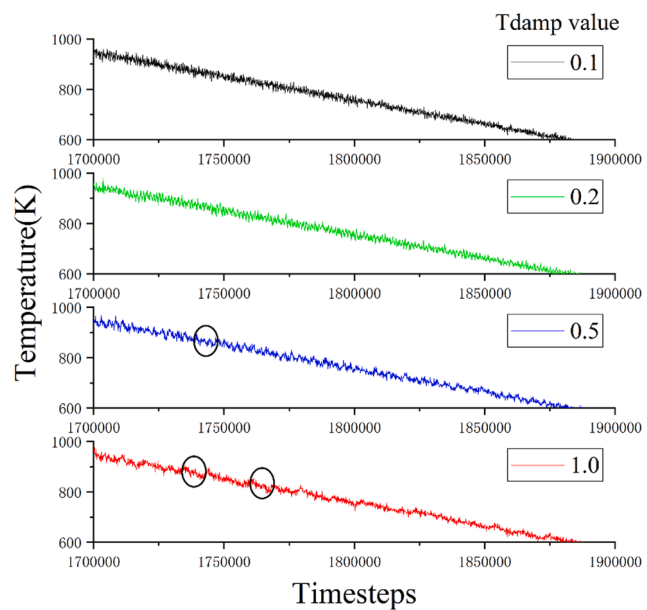


Fig. 7. Temperature vs timesteps diagram under different Tdamp values during solidification. The black circle indicates the temperature update cycle.

results show that part of FCC structures transform to HCP structures [28], resulting in its ratio reaches the maximum value of 66.4% in the final system. There are almost no ICO (icosahedron) crystal structures formed in all simulations of different Tdamp values during solidification.

In the cooling process, when the temperature is suitable for nucleation between atoms. There are many types of crystal structures forming, and the conversion relationships exists between crystal structures. However, it is not clear which type of crystal structure is formed first, only the change of the ratio of disordered atoms can explain the beginning of crystallization. Therefore, the decreasing ratio of disordered atoms is the best choice to judge the crystallization temperature.

The enlarged diagram of structure ratio vs temperature of the disordered atoms at range of 650–950 K is shown in Fig. 6. From Fig. 6, it shows that the crystallization temperature elevates with the decrease of Tdamp values, the crystallization temperature corresponds to 778.5 K, 814.4 K, 825.4 K and 844.8 K, respectively. These crystallization temperature are close to 820 K at which the BCC structures start to transform to HCP martensite [16].

In order to clarify the change of temperature during solidification. Temperature vs timesteps diagram is shown in Fig. 7.

From Fig. 7, it can be seen that the system with a larger Tdamp value requires more time to balance the temperature because of the greater fluctuation during temperature update period. The temperature is higher than the average value at the beginning of temperature update cycle. The peak of temperature elevates with the increase of Tdamp value, which corresponds to a higher crystallization temperature. At the end of the temperature update cycle, the temperature is lower than the average value. Temperature fluctuation causes temperature gradient, which is related to supercooling. We all know that local supercooling is beneficial to crystallization during the solidification process, resulting in the system with Tdamp value of 1.0 is a larger transformation ratio of crystal structure than other systems.

The CNA diagram of the different Tdamp values corresponding to the system after relaxation at 300 K for 20 ps is shown in Fig. 8. It is not difficult to find that the total crystal structures ratio rises with the increase of Tdamp value. Thereby, a larger Tdamp value is more conducive to the crystallization of atoms during the solidification process.

Above all, Tdamp values only influent evolution of crystal structure during the solidification process, but it's almost no effect on the melting

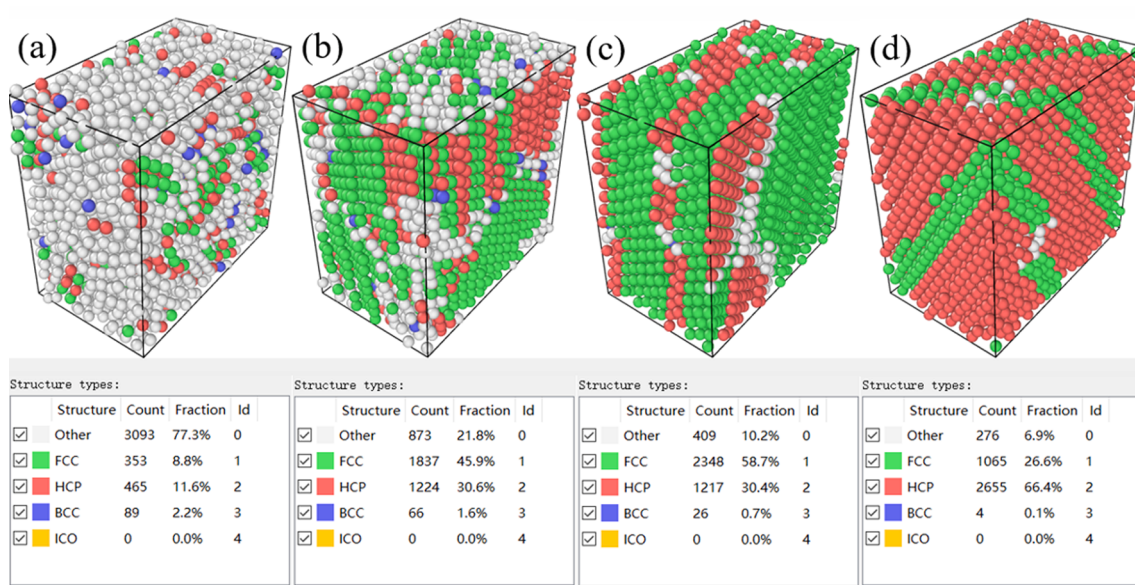


Fig. 8. The CNA diagram of the different Tdamp values corresponding to the system after relaxation at 300 K for 20 ps. Tdamp value of (a) 0.1; (b) 0.2; (c) 0.5; (d) 1.0, respectively.

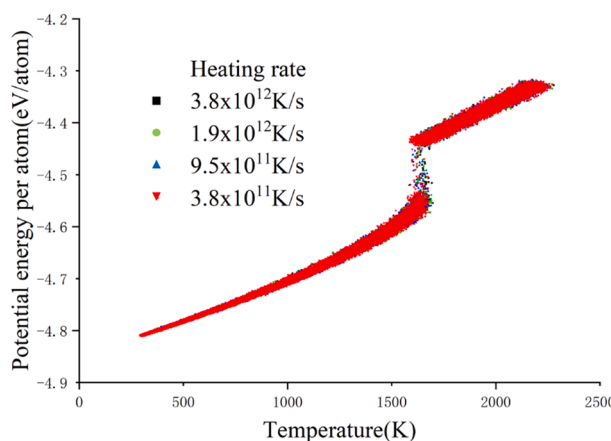


Fig. 9. Average atomic potential energy vs temperature diagram under different heating rates.

point. In many papers, the potential energy vs temperature diagram shows the S-shaped at the melting point. The reason can be explained that the Tdamp value is too large for the current simulation. For the real situation, only one Tdamp value is suitable. Other values are not appropriate. According to the S-shape of average atomic potential energy jump at melting point, it can be interpreted that the fluctuation of temperature caused by the insufficiency of energy provided by heater under a larger Tdamp value system. Finally, it is verified that the average atomic potential energy vertical jump is suitable for the current simulation system. In our work, an optimization method is proposed to obtain a suitable Tdamp value for simulation.

3.2. Heating/cooling rates

3.2.1. Influence of heating rates on crystal structure evolution and the melting point

In this section, the evolution of crystal structure of Ti under different heating rates is researched. The suitable Tdamp value of 0.1 is used for simulation. The average atomic potential energy vs temperature is

shown in Fig. 9.

From Fig. 9, the results show that heating rate has almost no effect on the shape of average atomic potential energy vs temperature curve, except for the melting point slightly increases under a higher heating rate. Considering the relationship between atomic potential energy and crystal structure, the crystal structure ratio vs temperature during the heating process is shown in Fig. 10.

From Fig. 10 (a, b), it can be seen that the type of crystal structure mainly transforms from HCP to Other in the whole heating process, and the ratio of disordered atoms increases with the elevated temperature. For observe carefully, the enlarged diagram of Fig. 10 (a, b) at the temperature range of 1400–1900 K is shown in Fig. 10 (c, d). It is found that the crystal structure ratio has a high degree of overlap, except the sharply changes of crystal structure at melting point, where the HCP (ratio about 12%) structures suddenly transform to disordered atoms. The higher heating rate slightly increases the melting point of Ti.

3.2.2. Influence of cooling rates on crystal structure evolution and the crystallization temperature

In order to alleviate the influence of hysteresis effect [29] on the evolution of the crystal structure during the solidification process, the Tdamp value of 0.1 is used for simulation. Firstly, the relationship between potential energy and temperature is shown in Fig. 11.

From Fig. 11, it is found that the lower the cooling rate, the more obvious decrease of average atomic potential energy during the solidification process, resulting in the lower average atomic potential energy in the final system. The change of potential energy is related to the evolution of crystal structure. Thereby, the corresponding crystal structure ratio vs temperature diagram is shown in Fig. 12. The average atomic potential energy of Other > FCC > HCP [16]. Hence, the change trend of disordered atomic potential energy in Fig. 11 is similar to the Fig. 12 (a) during the solidification process.

From Fig. 12, it is found that the ratio of transition from disordered state to crystal structure increases with the decrease of cooling rate. This phenomenon also appeared in the molecular dynamics study of nanopowders under different cooling rates [14]. It is difficult to crystal for disordered atoms at a higher cooling rate, due to crystallization requires enough time to release energy to nucleation. Higher rate results in lower energy transmission between system and thermostat, and produce significant hysteresis effect [29]. The crystallization of amorphous (disordered atoms) is a process of atom diffusion, where atoms in an unstable

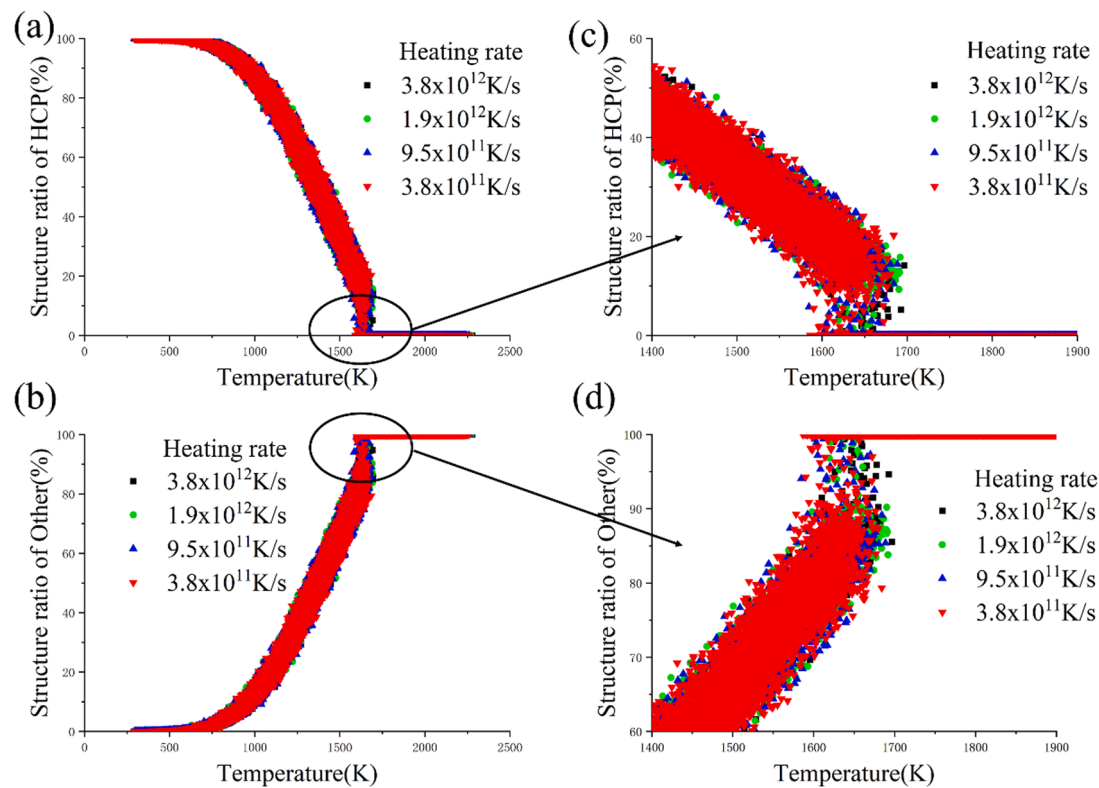


Fig. 10. (a, b) crystal structure ratio vs temperature diagrams corresponding to the different heating rates. (c, d) enlarged view of (a, b) at 1400–1900 K, respectively.

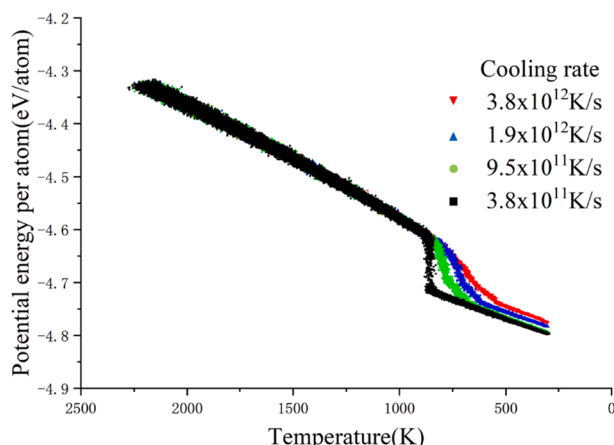


Fig. 11. average atomic potential energy vs temperature diagram under different cooling rates.

state are activated under the driving of heat energy and then they diffuse to the locations in which their energy is minimum [26]. According to the classical nucleation theory, nucleation is a random process caused by thermal activation and has nothing to do with homogeneous and heterogeneous nucleation [30,31]. Also, it is the evidence that thermally activated nucleation occurs in the MD simulation [32]. In particular, it has been confirmed that the relationship between the nucleation rate and temperature is nose-like shape, the reason is the competing effect between the two [30,33]. During the crystallization of metals, the nucleation rate of crystals is related to the supercooling. The short-range ordered arrangement of atoms caused by energy fluctuations and structural fluctuations near the crystallization temperature, which are the important factors for nucleation [20]. As the degree of supercooling

increase, on the one hand, it can promote the nucleation of atoms in a certain range [34]. On the other hand, a higher cooling rate has a negative effect on diffusion of atoms and inhibits the growth of crystal.

Fig. 12 shows that the condition with a large cooling rate (3.8×10^{12} K/s), the atoms are tough to nucleate and grow in a short period because of the constraint of insufficient time during the cooling process. Therefore, there is amount of amorphous structures formed which internal state is also unstable. During the relaxation, some disordered atoms continuously transform into HCP crystal structure which shows that sufficient time required for the cooling system to reach equilibrium at a higher cooling rate. When the cooling rate reduces to 1.9×10^{12} K/s, the ratio of crystal structures has great changes during the cooling process, which mainly manifests in obvious increase of FCC structures and a significant decrease of HCP structures. In this condition, the crystal structures tend to form FCC. Further decreasing cooling rate to 9.5×10^{11} K/s, the ratio of crystal structure of FCC decreases and the HCP increases. When the cooling rate reduces to 3.8×10^{11} K/s, the speed of transformation of crystal structure is accelerated, and quickly finished in a narrow temperature range. It indicates the rapid transformation from Other to HCP structure. In addition, a small amount of FCC crystal structures is formed then disappears rapidly during the transformation process. Which is an evidence of the structural transition from FCC to HCP. However, at different cooling rates, a small amount of BCC crystal structure is formed in the solidification process, and the ratio is between 2% and 4%, which has little effect on the simulation results. Therefore, there is no detailed analysis for it.

The crystallization temperature strongly depends on the cooling rate, and sufficient time is required to release heat for nucleation during the solidification process [29]. In Fig. 13, it shows a decreasing trend to crystallization temperature when the cooling rate increase. A higher cooling rate causes a decrease in the heat energy transfer between system and thermostat, which leads to a significant hysteresis effect [29], resulting the crystallization temperature declines with the increase of cooling rate.

The CNA diagram of the different cooling rates corresponding to the

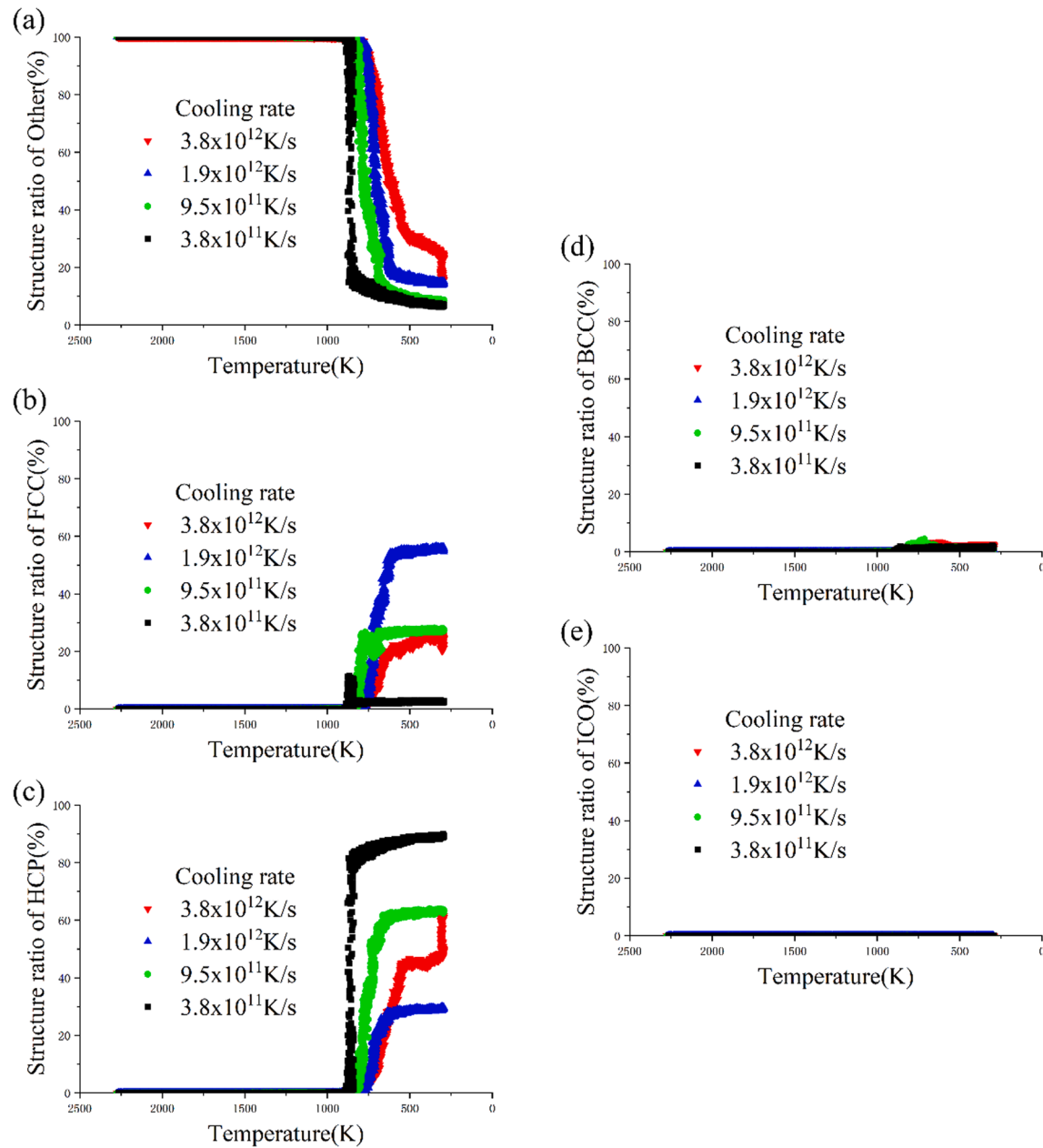


Fig. 12. Crystal structure ratio vs temperature diagrams under different cooling rates.

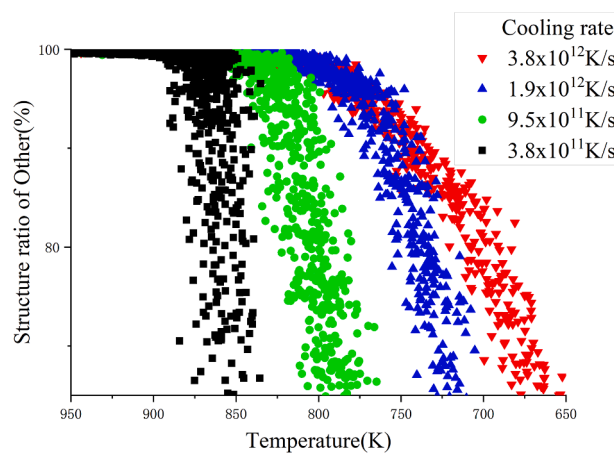


Fig. 13. Magnification diagram of structure ratio vs temperature of disordered atoms, which starts to transform into crystal structure under different cooling rates. The crystallization temperature decreases with the increase of cooling rate. (black corresponds to 892.4 K, green corresponds to 852.3 K, blue corresponds to 826.3 K, red corresponds to 805.1 K).

system after relaxation for 20 ps at 300 K is shown in Fig. 14. From the Fig. 14, it is found that the ratio of disordered atoms in the final system decreases with the cooling rate down, which indicates the disordered atoms are more conducive to crystal under a lower cooling rate.

4. Conclusions

In this work, MD was used to study the structural evolution of Ti atoms under different Tdamp values and heating/cooling rates. A series of simulations has been performed and the following results are summarized.

- (1) It is found that the atoms in a larger Tdamp value system are heated to the melting point, due to the insufficient energy supplied from the heater which causing the kinetic energy of system

decrease, and a phenomenon of S-shaped potential energy jump will appear in the potential energy vs temperature diagram. What's more, A larger Tdamp value is beneficial to the crystallization of the disordered atoms during solidification process. The Tdamp value causing the S-shape curve has almost no effect on melting point, but greatly influent the evolution of crystal structure during solidification process. For the real situation, only one Tdamp value is suitable for current simulation. In our work, four groups Tdamp values corresponding to their evolution of crystal structure and average atom potential energy with temperature have been researched, which provides a reference for optimizing Tdamp value to suit the current simulation. The results show that an appropriate Tdamp value corresponds to vertical jump of atomic potential energy at the melting point, and its value corresponds to 0.1 in the paper.

- (2) A higher heating rate slightly increases the melting point, but it has almost no effect on the evolution of crystal structure during the melting process. However, at higher cooling rate, disordered atoms are not conducive to the formation of crystal structure, but easy to form amorphous structure. In addition, the crystallization temperature drops with the increase of cooling rate. The reason is the hysteresis effect caused by cooling rate, resulting in the higher cooling rate system needs more longer time to release heat during the solidification process. In conclusion, a lower cooling rate is beneficial to the crystal structure formation of Ti atoms.

CRediT authorship contribution statement

Juze Jiang: Writing - original draft, Conceptualization, Software, Formal analysis, Visualization. **Xiaoxun Zhang:** Resources, Supervision, Funding acquisition. **Fang Ma:** Supervision, Funding acquisition. **Sensen Dong:** Project administration, Visualization. **Wei Yang:** Methodology. **Minghui Wu:** Software, Methodology.

Declaration of Competing Interest

The authors declare that they have no known competing financial interests or personal relationships that could have appeared to influence the work reported in this paper.

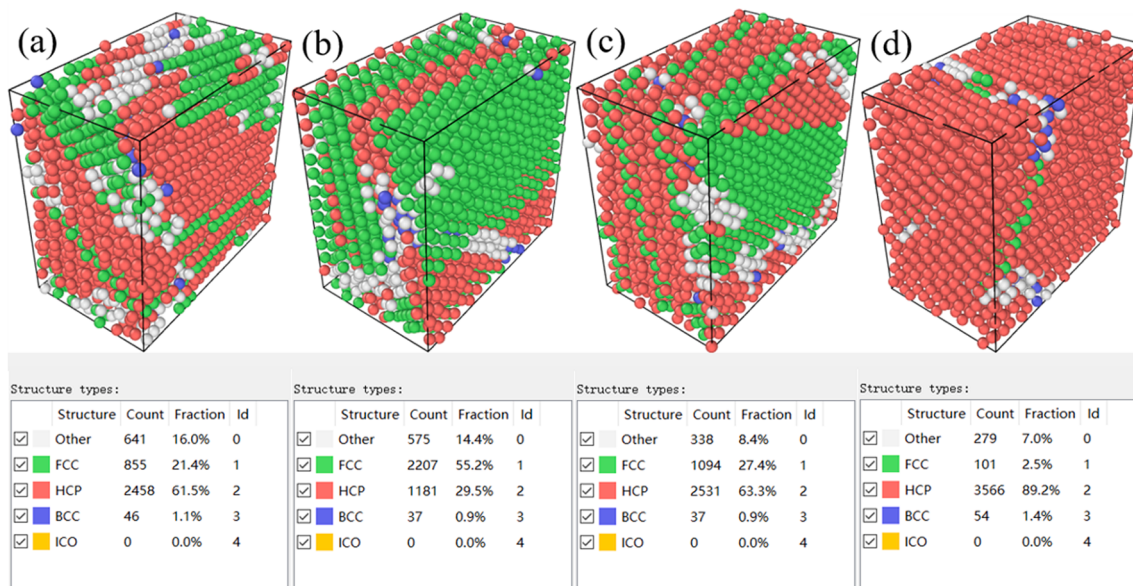


Fig. 14. The CNA diagram of the different cooling rates corresponding to the system after relaxation for 20 ps at 300 K (a) $3.8 \times 10^{12} \text{ K/s}$; (b) $1.9 \times 10^{12} \text{ K/s}$; (c) $9.5 \times 10^{11} \text{ K/s}$; (d) $3.8 \times 10^{11} \text{ K/s}$, respectively.

Acknowledgements

This work was financially supported by National Natural Science Foundation of China under Grant No. 51805313 and Industry-University-Research Collaboration Project between Shanghai University of Engineering Science and PMG 3D Technologies (Shanghai) Co., Ltd.

References

- [1] B. Zhang, H. Liao, C. Coddet, Microstructure evolution and density behavior of CP Ti parts elaborated by Self-developed vacuum selective laser melting system, *Appl. Surf. Sci.* 279 (2013) 310–316.
- [2] H. Attar, L. Löber, A. Funk, M. Calin, L.C. Zhang, K.G. Prashanth, S. Scudino, Y. S. Zhang, J. Eckert, Mechanical behavior of porous commercially pure Ti and Ti-TiB composite materials manufactured by selective laser melting, *Mater. Sci. Eng., A* 625 (2015) 350–356.
- [3] A. Ataei, Y. Li, C. Wen, A comparative study on the nanoindentation behavior, wear resistance and in vitro biocompatibility of SLM manufactured CP-Ti and EBM manufactured Ti64 gyroid scaffolds, *Acta Biomater.* 97 (2019) 587–596.
- [4] Q. Xu, W. Li, J.X. Zhou, Y.J. Yin, H. Nan, X. Feng, Molecular dynamics study on void collapse in single crystal hcp-Ti under hydrostatic compression, *Comput. Mater. Sci.* 171 (2020), 109280.
- [5] T. Wang, Y.Y. Zhu, S.Q. Zhang, H.B. Tang, H.M. Wang, Grain morphology evolution behavior of titanium alloy components during laser melting deposition additive manufacturing, *J. Alloy. Compd.* 632 (2015) 505–513.
- [6] B. Dutta, F.H. Froes, The Additive Manufacturing (AM) of titanium alloys, *Met. Powder Rep.* 72 (2) (2017) 96–106.
- [7] H. Attar, K.G. Prashanth, A.K. Chaubey, M. Calin, L.C. Zhang, S. Scudino, J. Eckert, Comparison of wear properties of commercially pure titanium prepared by selective laser melting and casting processes, *Mater. Lett.* 142 (2015) 38–41.
- [8] J.W. Liu, Q.D. Sun, C.A. Zhou, X.B. Wang, H. Li, K. Guo, J. Sun, Achieving Ti6Al4V alloys with both high strength and ductility via selective laser melting, *Mat Sci Eng A-Struct* 766 (2019), 138319.
- [9] F.A. Celik, A.K. Yildiz, Molecular dynamics simulation of crystallization kinetics and homogenous nucleation of Pt-Rh alloy, *J. Non-Cryst. Solids* 415 (2015) 36–41.
- [10] B.Y. Yu, Y.C. Liang, Z.A. Tian, Y.H. Zhang, Q. Xie, T.H. Gao, Y.F. Mo, MD study on topologically close-packed and configuration entropy of Mg40Al60 metallic glasses under rapid solidification, *J. Non-Cryst. Solids* 522 (2019), 119578.
- [11] L.W. Xiu, F.B. Jing, X. Zhang, Rapid solidification and crystal growth of Au3Ag alloy by MD simulation, *Mater. Sci. Eng., A* 298 (1–2) (2001) 262–267.
- [12] M. Avik, A.Z. Mohsen, Effects of solidification defects on nanoscale mechanical properties of rapid directionally solidified Al-Cu Alloy: A large scale molecular dynamics study, *J. Cryst. Growth* 527 (2019), 125255.
- [13] M. Azadeh, M. Kateb, P. Marashi, Determining phase transition using potential energy distribution and surface energy of Pd nanoparticles, *Comput. Mater. Sci.* 170 (2019), 109187.
- [14] S. Safaltn, S. Gürmen, Molecular dynamics simulation of size, temperature, heating and cooling rates on structural formation of Ag-Cu-Ni ternary nanoparticles (Ag34-Cu33-Ni33), *Comput. Mater. Sci.* 183 (2020), 109842.
- [15] S. Kurian, R. Mirzaifar, Selective laser melting of aluminum nano-powder particles, a molecular dynamics study, *Addit. Manuf.* 35 (2020), 101272.
- [16] G.J. Ackland, Theoretical study of titanium surfaces and defects with a new many-body potential, *Philos. Mag. A* 66 (6) (1992) 917–932.
- [17] M.I. Mendelev, T.L. Underwood, G.J. Ackland, Development of an interatomic potential for the simulation of defects, plasticity, and phase transformations in titanium, *J. Chem. Phys.* 145 (15) (2016), 154102.
- [18] R.G. Hennig, T.J. Lenosky, D.R. Trinkle, S.P. Rudin, J.W. Wilkins, Classical potential describes martensitic phase transformations between the α , β , and ω titanium phases, *Phys. Rev. B* 78 (5) (2008), 054121.
- [19] A.T. Dinsdale, SGTE data for pure elements, *Calphad* 15(4) 317–425.
- [20] A. Samanta, M.E. Tuckerman, T.Q. Yu, W. E, Microscopic mechanisms of equilibrium melting of a solid, *Science* 346(6210) (2014) 729–32.
- [21] W. Hayami, First-order polyamorphic phase transition in boron nitride, *J. Non-Cryst. Solids* 456 (2017) 132–137.
- [22] Y.Y. Zhu, H. Wang, L.K. Wu, M. Li, From first to second order nonequilibrium phase transition in crystal-amorphous interface: Effects of spatial and kinetic constraints, *J. Alloy. Compd.* 850 (2021), 156841.
- [23] S.T. Oyinbo, T.-C. Jen, Molecular dynamics investigation of temperature effect and surface configurations on multiple impacts plastic deformation in a palladium-copper composite metal membrane (CMM): A cold gas dynamic spray (CGDS) process, *Comput. Mater. Sci.* 185 (2020), 109968.
- [24] S. Ma, S. Li, T. Gao, Y. Shen, X. Chen, C. Xiao, T. Lu, Molecular dynamics simulations of structural and melting properties of Li₂SiO₃, *Ceram. Int.* 44 (3) (2018) 3381–3387.
- [25] H.G. Abbas, J.R. Hahn, Crystallization mechanism of liquid tellurium from classical molecular dynamics simulation, *Mater. Chem. Phys.* 240 (2020), 122235.
- [26] Y. Zhang, S. Jiang, Atomistic mechanisms for temperature-induced crystallization of amorphous copper based on molecular dynamics simulation, *Comput. Mater. Sci.* 151 (2018) 25–33.
- [27] T. Abe, S. Akiyama, H. Onodera, Crystallization of Sputter Deposited Amorphous Ti-52at%Al Alloy, *ISIJ Int.* 34 (5) (1994) 429–434.
- [28] Q.X. Pei, C. Lu, H.P. Lee, Crystallization of amorphous alloy during isothermal annealing: a molecular dynamics study, *J. Phys.: Condens. Matter* 17 (10) (2005) 1493–1504.
- [29] Y.C. Zou, S.K. Xiang, C.D. Dai, Investigation on the efficiency and accuracy of methods for calculating melting temperature by molecular dynamics simulation, *Comput. Mater. Sci.* 171 (2020), 109156.
- [30] T. Fujinaga, Y. Shibuta, Molecular dynamics simulation of athermal heterogeneous nucleation of solidification, *Comput. Mater. Sci.* 164 (2019) 74–81.
- [31] B.R. Manon, P. Thomas, Å. John, Kinetic theory of nucleation in multicomponent systems: An application of the thermodynamic extremum principle, *Acta Mater.* 171 (2019) 1–7.
- [32] A.O. Tipeev, E.D. Zanotto, Nucleation kinetics in supercooled Ni50Ti50: Computer simulation data corroborate the validity of the Classical Nucleation Theory, *Chem. Phys. Lett.* 735 (2019), 136749.
- [33] S.C.C. Prado, J.P. Rino, E.D. Zanotto, Successful test of the classical nucleation theory by molecular dynamic simulations of BaS, *Comput. Mater. Sci.* 161 (2019) 99–106.
- [34] Y. Sun, F. Zhang, L. Yang, Z. Ye, H.J. Song, M.I. Mendelev, C.Z. Wang, K.M. Ho, Effect of samarium doping on the nucleation of fcc-aluminum in undercooled liquids, *Scr. Mater.* 154 (2018) 202–206.